6. V. Ya. Neiland, "Toward a theory of separation of a laminar boundary layer in a supersonic flow," Izv. Akad. Nauk SSSR, Mekh. Zhidk. Gaza, No. 4 (1969).
7. K. Stewartson and P. G. Williams, "Self-induced separation," Proc. R. Soc. London Ser. A, 312, No. 1509 (1969).
8. V. V. Sychev, "On laminar separation," Izv. Akad. Nauk SSSR, Mekh. Zhidk. Gaza, No. 3 (1972).
9. I. I. Lipatov, "Detachment of the boundary layer in the uniform injection of gas into a supersonic flow," Tr. TsAGI, No. 1864 (1977).
10. W. D. Hayes and R. F. Probstein (eds.), Hypersonic Flow Theory, 2nd Ed., Academic Press (1967).
11. G. G. Chernyi, Gas Flows with a High Supersonic Velocity [in Russian], Fizmatgiz, Moscow (1959).
12. V. Ya. Neiland, "Propagation of disturbances upflow in the interaction of a hypersonic flow with a boundary layer," Izv. Akad. Nauk SSSR, Mekh. Zhidk. Gaza, No. 4 (1970).
13. G. N. Dunin and D. O. Lyzhin, "One method of calculting the regime of strong viscous interaction on a delta wing," Izv. Akad. Nauk SSSR, Mekh. Zhidk. Gaza, No. 4 (1983).
14. A. A. Kovalenko, "Study of boundary-layer separation in an interaction with a hypersonic gas flow," Uchen. Zap. TsAGI, 5, No. 6 (1974).

EFFECT OF RAREFACTION AND THE TEMPERATURE FACTOR ON THE STRUCTURE AND PARAMETERS OF SUPERSONIC UNDEREXPANDED JETS OF A MONATOMIC GAS

V. A. Ivanov, G. A. Luk'yanov,
and I. V. Shatalov

UDC 533.6.011.8

The pattern of flow in an underexpanded supersonic jet discharged into a submerged space is determined in the general case by several dimensionless parameters which characterize conditions on the edge of the nozzle and in the surrounding medium. If we limit ourselves to the discharge of a monatomic gas from a sonic nozzle into the same gas, then the number of governing parameters is reduced to three — the characteristic Reynolds number $Re_L = Re_*/N^{0.5}$, the degree of expansion $N = p_0/p_\infty$, and the temperature factor $\tau = T_0/T_\infty$, where Re_* is the Reynolds number calculated from the parameters in the critical section of the nozzle, p_0 and T_0 are the stagnation temperature and pressure, and p_∞ and T_∞ are the ambient pressure and temperature [1].

At $Re_L > 10^2$, a continuous flow regime is realized. Here, the effect of viscosity and the temperature factor on flow in the initial section of the jet is restricted to the outer mixing zone. An inviscid core with a shock-wave structure (SWS), including suspended and central shocks, is preserved inside the jet. Meanwhile, the suspended shock and the mixing layer are separated from each other by a zone of inviscid flow. Values of $Re_L < 10^2$ correspond to flow regimes characterized by merging of the shock zones, the compressed layers, and the mixing layers. With a decrease in Re_L, the effect of viscosity and the temperature factor increases and propagates upflow [1-4].

The study [2] examined the effect of the temperature factor on the flow pattern and structure of an underexpanded argon jet discharged from a sonic nozzle into a submerged space. Here, $Re_L = 10^3$-3, τ = 1-18, and N = 370-28,500. As the initial data, the authors used the density field obtained from electron—x-ray method. In the analysis of the experiments, most attention was paid to the range $Re_L = 10^3$-30.

In the present investigation, the ranges studied are expanded in the direction of smaller Re_L and large τ ($Re_L = 0.5$-10^2, τ = 1-38). Based on analysis of results obtained for underexpanded argon jets at $N > 10^2$ in these ranges of Re_L and τ, we discerned two characteristic subregions in the transient flow regime, with eroded and completely degenerate SWS's. We also observed a region of flow regimes in which density decreases monotonically. This region can be regarded as intermediate between the transient regime and the free-molecular regime. We studied the effect of Re_L and τ on the structure and characteristic geometric

Leningrad. Translated from Zhurnal Prikladnoi Mekhaniki i Tekhnicheskoi Fiziki, No. 6, pp. 62-67, November-December, 1987. Original article submitted September 4, 1986.

dimensions of the initial section of the jet, and we derived corresponding empirical relations which generalize the results.

High-temperature jets were generated by a dc electric-arc plasmatron, with vortical stabilization of the arc. The plasmatron was equipped with a circular sonic nozzle of the diameter $d_* = 4$ mm and was mounted on a three-component coordinate mechanism. The design of the plasmatron was similar to that described in [3]. A water-cooled receiver was attached to the plasmatron to create jets with $\tau = 4$-20, while jets with $1 < \tau \leq 4$ were created with the aid of a resistance heater. Stagnation temperature was monitored from the readings of thermocouples and calorimetric data. The discharge regimes corresponding to $\tau = 1$ were realized without an arc on the plasmatron. The upper limit of the range of T_0 was $T_0 \approx 10^4$ K, in order to keep relaxation processes from affecting the gasdynamic structure. According to the data in [3], in the investigated range of p_0 and T_0, ionization of argon still has no significant effect on the gasdynamics of expansion.

The electron beam was created by means of a serially produced system ÉOSS-2, with a VIP 2-50-60 high-voltage power source. The energy of the electrons was 20-25 keV, while the current of the beam was 1-5 mA. The characteristic x-rays created by the interaction of the electron beams with argon atoms were recorded with SRPO-16 and SI-12R proportional counters together with the SSD instrument counter. The locality of the measurements was 1 mm, and the density measurement error was no greater than 20%. The measurement method was similar to that described in [2].

Figures 1 and 2 show the results of density measurement along and across the jet. These results can be used to evaluate the effect of the parameters Re_L and τ on flow in the initial section of underexpanded submerged argon jets. In the figures, $\rho^0 = \rho N/\rho_0$, $x^0 = x/d_* N^{0.5}$, $y^0 = y/d_* N^{0.5}$, a shows data for jets at $\tau = 1$, and b shows the data obtained when $\tau = 35$. The straight line in Fig. 1 represents the axisymmetric, isentropic free expansion of the monatomic gas, while the dashed lines in Figs. 1 and 2 show profiles of density for jets of inviscid gas ($Re_L = \infty$). The data shown in Fig. 2 pertains to the cross section $x^0 = 0.44$.

A reduction in Re_L is accompanied by gradual erosion of the SWS, expansion of the mixing layers, and contraction of the region of isentropic free expansion. In the investigated range of Re_L, merging of the viscous mixing layer with the compressed layer and the shock waves means that the central shock (Mach cone) can no longer be regarded as an isolated shock wave. According to [4], the closure of the mixing layer in the region $x^0 \approx 0.65$ — where the Mach cone is located at $Re_L = \infty$ — corresponds to $Re_L = 30$-80. Thus, the compression seen on axial density profiles at $Re_L < 10^2$ is no longer compression at the normal shock, and the compression region can only formally be called a Mach cone. The compression region does not correspond to the flow pattern in a normal shock with regard to either geometry or internal structure. During the reduction in Re_L, the erosion of the central shock is preceded by erosion of the suspended shocks. This is quite evident, for example, from a comparison of the curves for $Re_L = 24$ in Figs. 1 and 2. Whereas the compression region corresponding to the eroded Mach cone is still readily detectable on the axial profiles, both the suspended shocks and the compressed layers as a whole have been almost completely eroded in the transverse profiles. Thus, with an increase in the degree of rarefaction, signs of the SWS disappear last from the axial region.

We should also point out the important difference in the mixing of jets at $\tau = 1$ and $\tau \gg 1$. In the first case, viscous dissipation erodes the relatively fine density peak in the compressed layer, while in the second case it erodes the narrow region of large positive pressure gradients in the radial direction. At $\tau = 1$, as Re_L decreases the density profiles are restructured in such a way that, at $Re_L \leq 8$-10, the density minimum on the axis which is characteristic of large Re_L disappears and density decreases monotonically with increasing distance from the nozzle edge. With an increase in τ, a transition to a regime with monotonically decreasing density is seen at lower Re_L. When τ is large, the positive axial and transverse density gradients in the mixing layers decrease with a decrease in Re_L but remain in existence throughout the investigated range of Re_L.

The rarefaction effects decrease with an increase in τ, while the dimensions of the undisturbed region of free expansion increase. The effect of τ on the longitudinal dimension of the free-expansion region is illustrated in Fig. 1. Comparison of the curves for identical Re_L and different τ shows that the region of isentropic free expansion is longer in the high-temperature jet. Here, the deviation from isentropic expansion is sharper at high τ than at $\tau = 1$. The latter circumstance is a result of the superposition of a mixing region with a high density gradient on the shock-compression region.

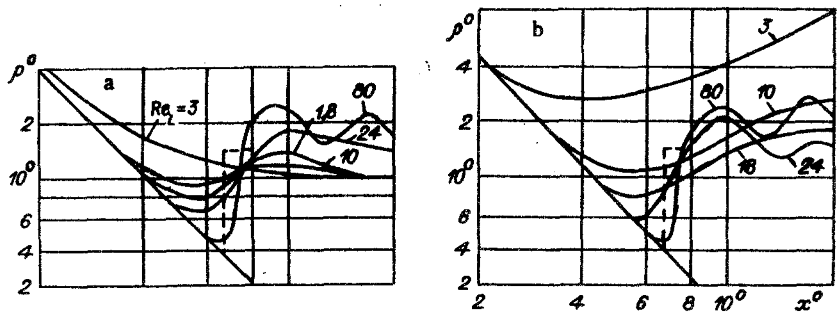

Fig. 1

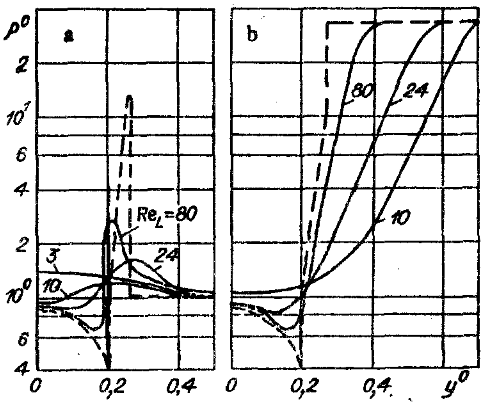

Fig. 2

The experimental data on the length of the region of isentropic free expansion L (the distance from the nozzle edge to the point on the jet axis where density deviates from the isentropic value by 10%) at $Re_L \geq 2$ is approximated by the formula

$$L/x_cF = (1 + 20/\mathrm{Re}_L)^{-1}.$$

Here, $F = 1 + 0.16(\tau - 1)/Re_L$; $x_c = 0.645 d_* N^{0.5}$ is the distance to the central shock in dense, highly underexpanded submerged jets at $M_a = 1$ [5].

The increase in the relative length of the free-expansion region L/x_c as τ increases at constant d_*, Re_L, and N is explained by the high density of heated jets. The conditions $Re_{L1} = Re_{L2}$, $N_1 = N_2$ — where the subscripts 1 and 2 pertain to high-temperature jets ($\tau_1 > 1$) and jets with $T_0 = T_\infty$ ($\tau_2 = 1$) — lead to the equality $\mathrm{Re}_{*1} = \mathrm{Re}_{*2}$ ($\mathrm{Re}_* = v_* \rho_* d_* / \mu_*$, where v_* and μ_* are the velocity and viscosity of the gas in the critical section of the nozzle). At $T_0 < 10^4$ K, it can be approximately assumed for argon that $v_* \sim T_0^{0.5}$, $\mu_* \sim T_*^m$, $m \approx 0.75$ [6]. As a result, we obtain $\rho_{*1}/\rho_{*2} = (T_{01}/T_{02})^{0.25}$.

Within the free-expansion region, density on the jet axis is determined by the relation [1] $\rho/\rho_0 = B(\gamma, M_a)(x/d_*)^{-2}$. With allowance for the equality of N, the densities on the axes of jets 1 and 2 at the distance $x_1/d_{*1} = x_2/d_{*2}$ are connected by the relation $\rho_1/\rho_{01} = \rho_2/\rho_{02}$. From here, with allowance for $T_{\infty 1} = T_{\infty 2} = 300$°K, $\rho_1/\rho_2 = \rho_{01}/\rho_{02} = (T_{01}/T_{02})^{0.25} = \tau^{0.25}$. In this case, the ratio of the densities of the gas and the undisturbed medium $\rho_{\infty 1}/\rho_{\infty 2} = (T_{01}/T_{02})^{1.25} = \tau_1^{1.25}$.

Thus, at Re_L = const, N = const, and d_* = const, a heated jet turns out to be denser than a cold jet. This is true both inside the inviscid internal flow and in the viscous outer mixing zone.

Analysis of the experimental data obtained here makes it possible, within the investigated ranges of the parameters, to distinguish two characteristic subregions in the transient flow regime. These subregions are characterized by different degrees of rarefaction, or different relative roles for the processes associated with shock waves and viscous dissipation. We can also distinguish a region of flow regimes (with density monotonically decreasing downflow) which corresponds to an even higher degree of rarefaction. Region II, corresponding to jets with an eroded SWS, is found in the plane of the parameters τ and Re_L (Fig. 3) to the left of the region corresponding to the continuous flow regime I. The main indicator allowing us to identify this region is the presence of a wavy density change on the axial profile in the vicinity of the eroded Mach cone (accurate to within 10%). Inside region II, the

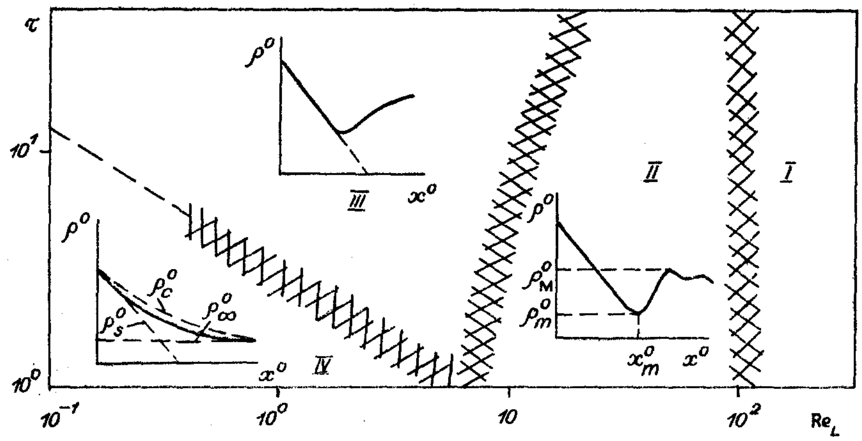

Fig. 3

importance of shock-wave processes in the initial section of the jet changes from considerable at the boundary of regions I and II to negligible at the boundary of regions II and III. Region III includes regimes with a completely degenerate SWS.

In regions III and IV, the flow in the initial section consists of an inviscid internal zone of free expansion and a viscous external mixing zone. The flow is not affected by shock-wave processes. Region III is denser than region IV. An internal core which is rarefied relative to the surrounding medium is preserved in the jet within region III at $\tau > 1$. This core gradually disappears with a decrease in Re_L or τ. The flow regimes with monotonically increasing density belong to region IV, which can be regarded as being immediately adjacent to the region of free-molecular discharge of the jet into the submerged space. The latter region is characterized by a monotonic change in density. With sufficiently small values of ρ_∞ and large values of ρ_0, the density of the gas in the flow field is determined as the sum of the undisturbed densities of the jet component ρ_s^0 (corresponding to isentropic free expansion into a cavity) and the surrounding medium ρ_∞^0 (region IV):

$$\rho_c^0 = \rho_s^0 + \rho_\infty^0. \tag{1}$$

The accuracy of Eq. (1) increases as $Re_L \to 0$. Since ρ_s^0 decreases monotonically with increasing distance from the nozzle edge and ρ_∞^0 is constant, then ρ_c^0 decreases monotonically downflow to ρ_∞^0 from its value at the nozzle edge. In Fig. 4, the free-molecular limit for the axial density profile is represented by curve 6 ($\tau = 1.4$).

The limited capabilities of the experimental unit allowed us to demonstrate the transition from region II to region IV only for small τ. Figure 4 shows data depicting the typical restructuring of the axial density profiles at $\tau = 1.4$-2. Curves 1 ($Re_L = 40$, $\tau = 2$), 2 ($Re_L = 24$, $\tau = 1.7$), and 3 ($Re_L = 10$, $\tau = 1.55$) pertain to region II, while curves 4 ($Re_L = 3.3$, $\tau = 1.4$) and 5 ($Re_L = 0.5$, $\tau = 1.4$) pertain to regions III and IV.

Flow regimes with eroded and completely degenerate SWS's can be regarded as an analog of the regimes associated with the "diffuse" and transitional layers realized in the flow of a low-density gas about a body [7]. The flow regimes belonging to region IV correspond to a nearly free-molecular regime.

Let us look at certain features of the above regimes in more detail. Figure 5 shows data on the dependence of the minimum density ρ_m^0 (see Fig. 3) on Re_L for $\tau = 1$, 4, and 35. In the range of Re_L corresponding to region II, the effect of τ on ρ_m^0 is small. The transition from region II to region III is accompanied by stratification of the curves $\rho_m^0 = f(Re_L)$ in relation to τ. With an increase in τ, the beginning of the stratification is shifted toward large Re_L, while the transition to the regime with a monotonic change in density is shifted toward small Re_L. With a maximum error of 15%, the distance from the nozzle edge to the point on the axis where the density minimum is reached x_m^0 (regions II and III) is independent of τ and at $Re_L \geq 1$ is approximately described by the formula $x_m/x_c = Re_L/(3 + Re_L)$.

Figure 6 shows data on the compression $\varepsilon = \rho_M^0/\rho_m^0$ (region II) in the zone where the Mach cone is eroded. At $Re_L > 10^2$, $\varepsilon = 4$. This case corresponds to the limiting compression on a normal shock for a monatomic gas. With a decrease in Re_L to 60-80, ε increases to 5-5.5. A further reduction in Re_L is accompanied by thickening of the compression zone and a reduction in ε. At a fixed value of Re_L, an increase in τ is accompanied by a reduction in ρ_m^0 and

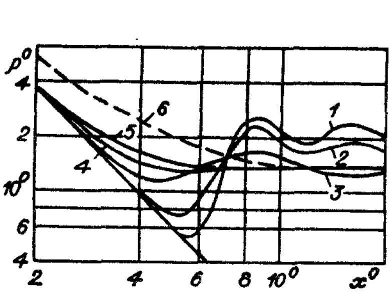

Fig. 4

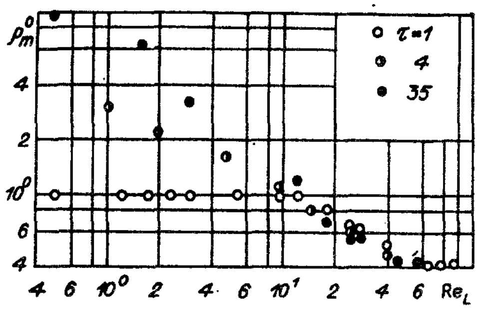

Fig. 5

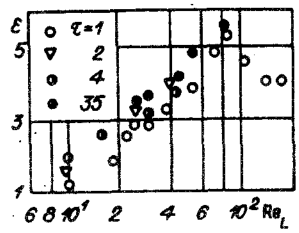

Fig. 6

an increase in ρ_M^0, which leads to an increase in ε. Determination of ε makes sense only within region II, where the eroded SWS is still present. At values of τ differing appreciably from unity, the shock-compression region is seen up to Re_L = 8-10, while ε gradually approaches unity with a decrease in Re_L. In the case $\tau \gg 1$, large transverse density gradients cause the mixing layer to interact with the shock-compression region in such a way that the downflow part of the compression region (where ρ_M^0 is attained) turns out to be very indistinct while its front part retains its characteristics. In region II, along with the value of ε it is important to know the thickness of the compression region δ along the jet axis. As in [8], we determine δ from the relation $\delta = (\rho_M - \rho_m)(\partial\rho/\partial x)_{max}$. To within 15%, experimental data on δ is independent on τ and is approximately generalized by the formula $\delta/x_c = 16/(20 + Re_L)$.

The distance from the nozzle edge to the inflection point on the density profile x_c', where the value of $(\partial\rho/\partial x)_{max}$ was determined, coincides with x_c at $Re_L > 10^2$. With a decrease in Re_L from 10^2 to 30, x_c' increases to $(1.2\text{-}1.3)x_c$. A further reduction in Re_L leads to a reduction in x_c' to $x_c' < x_c$.

LITERATURE CITED

1. V. G. Dulov and G. A. Duk'yanov, Gasdynamics of Discharge Processes [in Russian], Nauka, Novosibirsk (1984).
2. L. I. Kuznetsov, A. K. Rebrov, and V. N. Yarygin, "High-temperature argon jets of low density after a sonic nozzle," Zh. Prikl. Mekh. Tekh. Fiz., No. 3 (1975).
3. G. A. Luk'yanov, V. V. Nazarov, and V. V. Sakhin, "Structure of underexpanded jets of an argon plasma in the transient regime," Zh. Prikl. Mekh. Tekh. Fiz., No. 5 (1981).
4. V. V. Volchkov, A. V. Ivanov, et al., "Low-density jets after a sonic nozzle at large pressure gradients," Zh. Prikl. Mekh. Tekh. Fiz., No. 2 (1973).
5. S. Crist, R. M. Sherman, and D. R. Glass, "Study of the highly underexpanded sonic jet," AIAA J., 4, No. 1 (1966).
6. S. V. Dresvin (ed.), Physics and Engineering of Low-Temperature Plasmas [in Russian], Atomizdat, Moscow (1972).
7. W. D. Hayes and R. F. Probstein (eds.), Hypersonic Flow Theory, 2nd Ed., Academic Press (1967).
8. V. V. Volchkov and A. V. Ivanov, "Thickness and internal structure of a normal shock formed in the discharge of a highly underexpanded jet into a low-density space," Izv. Akad. Nauk SSSR, Mekh. Zhidk. Gaza, No. 3 (1969).